TRENDS IN SCIENCES 2026; 23(12): 13972
https://doi.org/10.48048/tis.2026.13972
RESEARCH ARTICLE

Synthesis and Computational Assessment of 2′,4-Dihydroxy-3-methoxychalcone in Comparison with A Structural Chalcone Isomer

Arfiani Nur[1,2], Nunuk Hariani Soekamto[1,*], Bambang Purwono[3], Herlina Rasyid[1], Ummi Zahra[2], Aisyah[2], Artati[4], Andi Nur Fitriani[5], Fadliah[6], M. Yasser[7], Muharram[8], Paulina Taba[1], Indah Raya[1], Abdul Wahid Wahab[1] and Najah Baroud[9]

[1]*Department of Chemistry, Faculty of Mathematics and Natural Sciences, Hasanuddin University, Makassar 90245, Indonesia*
[2]*Depatrment of Chemistry, Faculty of Science and Technology, Alauddin State Islamic University, Makassar 92118, Indonesia*
[3]*Department of Chemistry, Faculty of Mathematics and Natural Sciences, Gadjah Mada University, Yogyakarta 55281 Indonesia*
[4]*Makassar Ministry of Health Polytechnic, Makassar 90222, Indonesia*
[5]*Department of Chemistry, Faculty of Science, Universitas Muhammadiyah Bulukumba, South Sulawesi 92513, Indonesia*
[6]*Department of Mining Engineering, Faculty of Earth and Energy Technology, Trisakti University, Jakarta 11440, Indonesia*
[7]*Department of Chemical Engineering, Politeknik Negeri Ujung Pandang, South Sulawesi 90245, Indonesia*
[8]*Department of Chemistry, Universitas Negeri Makassar, South Sulawesi 90224, Indonesia*
[9]*Department of Chemistry Education, Faculty of Science, University of Zawia, Al Zawia 16418, Libya*

([*]Corresponding author's e-mail: nunukhariani@unhas.ac.id)

Received: 1 April 2026, Revised: 6 May 2026, Accepted: 13 May 2026, Published: 10 July 2026

Abstract

Chalcone derivatives' varied biological activity and structural adaptability have drawn a lot of interest. This study synthesized 2′,4-dihydroxy-3-methoxychalcone by Claisen-Schmidt condensation and compared it to its positional isomer, 4′,4-dihydroxy-3′-methoxychalcone. Elucidation of chemical structure based on FTIR, ^{1}H-NMR, ^{13}C-NMR and GC-MS spectroscopic characterization. Molecular docking analysis was employed to investigate interactions with major anti-apoptotic members of the Bcl-2 protein family, while energy minimization was conducted to assess complex stability. *In silico* toxicity prediction was also performed to estimate acute toxicity profiles. The results showed that both chalcone isomers exhibited favorable binding affinities toward proteins belongingto the Bcl-2 family, particularly Bcl-xL, and formed stable ligand-protein complexes after energy minimization. Predicted LD_{50} values indicated low acute toxicity for both compounds. Overall, these findings suggest that structural isomerism influences molecular interactions with apoptosis regulating proteins and support futher investigation of hydroxy-methoxychalcones in antitumor-related studies.

Keywords: 2′,4-Dihydroxy-3-methoxychalcone, Chalcone isomers, Molecular docking, Bcl-2 family proteins, Drug-likeness, *In silico* toxicity

Introduction

Chalcones, characterized by an α,β-unsaturated carbonyl framework, represent an important class of naturally inspired compounds with broad pharmacological relevance [1,2]. As key intermediates in flavonoid biosynthesis, chalcones have been extensively investigated for their anticancer potential,

antioxidant and anti-infalmmatory properties [3]. Variations in chemical structure, particularly hydroxyl and methoxy substitutions, have been shown to significantly influence their biological performance, making chalcones attractive scaffolds for rational drug design [4,5].

Among chalcone derivatives, hydroxy- and methoxy-substituted compounds have shown notable cytotoxic effect against several cancer cell lines, primarily through apoptosis induction. Notably, 2′,4-dihydroxy-3-methoxychalcone has been previously reported to inhibit the proliferation of cancer cells and trigger apoptotic pathways in cervical and colon cancer models [6]. However, despite its promising bioactivity, comprehensive evaluations integrating physicochemical properties, pharmacokinetics, and molecular interactions with apoptosis-regulating proteins remain limited.

Among the apoptosis-regulating proteins, the Bcl-2 family plays a central role in controlling the intrinsic mitochondrial apoptotic pathway by regulating mitochondrial outer membrane permeabilization and cytochrome c release [7,8]. Anti-apoptotic members such as Bcl-2, Bcl-xL, Mcl-1, Bcl-w, and Bfl-1 prevent apoptosis by binding and sequestering pro-apoptotic proteins, thereby promoting cancer cell survival [7,9]. Bcl-xL is particularly relevant in anticancer drug discovery because its high expression has been associated with apoptosis resistance, tumor cell survival, and reduced response to anticancer therapy [9,10]. In addition, natural chalcones have been reported to interact with the BH3-binding groove of anti-apoptotic Bcl-2 family proteins, including Bcl-2, Bcl-xL, and Mcl-1, supporting their potential role as apoptosis-modulating anticancer agents [11]. Therefore, evaluating the interaction of chalcone derivatives with Bcl-xL and related anti-apoptotic proteins may provide useful insight into their potential mechanism as apoptosis-inducing anticancer agents.

Subtle positional variations of hydroxyl groups can significantly alter solubility, membrane permeability, protein binding affinity, and overall drug-likeness [12,13]. Nevertheless, comparative studies addressing the impact of such positional isomerism on the antitumor potential of chalcones are scarce. This knowledge gap hampers the rational optimization of chalcone-based therapeutics and underscores the need for integrative studies combining synthetic chemistry and computational modeling.

Recent advances in *in silico* drug discovery tools provide an efficient platform for early-stage evaluation of molecular behavior, enabling rapid screening of drug-likeness, target affinity, and toxicity profiles prior to experimental validation. However, these computational approaches have rarely been applied to systematically compare structurally related chalcone isomers with established anticancer potential.

Therefore, this study aims to synthesize 2′,4-dihydroxy-3-methoxychalcone and conduct a comprehensive computational assessment of its drug-likeness, pharmacokinetic properties, molecular interactions with Bcl-2 family proteins, and predicted toxicity, in comparison with 4′,4-dihydroxy-3′-methoxychalcone. The findings are expected to offer mechanistic understanding of structure–activity relationships and facilitate the development of chalcone-derived antitumor agents.

Materials and methods

Materials

Analytical grade substances were utilized in this investigation without additional purification. Vanillin and 2-hydroxyacetophenone were used as starting materials, while potassium hydroxide served as the base catalyst. Ethanol, methanol, hydrochloric acid, and distilled water were used as solvents during synthesis and purification. Reaction progress was monitored using thin-layer chromatography (TLC) on silica gel plates with a chloroform-petroleum ether solvent system. Analytical instruments included a melting point apparatus, FTIR spectrometer, and ^{1}H- and ^{13}C-NMR spectrometers. Computational analyses were performed using Open Babel, UCSF Chimera, CB-Dock2, Discovery Studio Visualizer, SwissADME, Swiss-PDB Viewer, and ProTox-II webserver.

Preparation of 2′,4-Dihydroxy-3-methoxychalcone

Vanillin and 2-hydroxyacetophenone experienced a Claisen-Schmidt condensation in ethanol to yield 2′,4-Dihydroxy-3-methoxychalcone. To speed up the condensation process, potassium hydroxide was introduced as a catalyst and the mixture was subjected to microwave irradiation (187 W for 25 min). After the

reaction was finished, the mixture was allowed to cool and subsequently neutralized with dilute hydrochloric acid until a neutral pH was achieved. To get the purified chalcone derivative, the precipitated solid was filtered, washed with cold distilled water, and recrystallized using a methanol-water mixture [14].

Ligand preparation

2′,4-dihydroxy-3-methoxychalcone together with 4′,4-dihydroxy-3′-methoxychalcone their three dimensional structures were retrieved in SDF format from the PubChem database. The ligand files were converted into PDB format using Open Babel software [15], and before docking analysis using UCSF Chimera [16], the ligand files were viewed to confirm structural integrity.

Drug-likeness and ADME prediction

Drug-likeness and pharmacokinetic properties of both chalcone isomers (**Figure 1**) were evaluated using the SwissADME web platform. The analysis included assessment of physicochemical properties, Lipinski's rule of 5 compliance, gastrointestinal absorption, solubility, and predicted bioavailability based on the canonical SMILES of each compound [17,18].

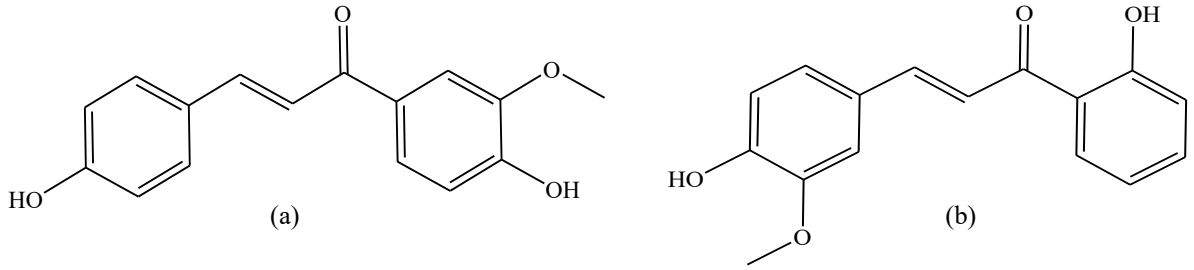


Figure 1 Molecular structures of 4',4-dihydroxy-3'-methoxychalcone (a) and 2',4-dihydroxy-3-methoxychalcone (b).

Swiss ADME evaluation of the ligand

Assessment of drug candidacy requires consideration of fundamental pharmacokinetic characteristics, particularly absorption, distribution, metabolism, and excretion (ADME) [19]. SwissADME is a widely used computational platform that enables rapid evaluation of drug-likeness, physicochemical characteristics, pharmacokinetic behavior, and medicinal chemistry properties through an interpretable output framework. In the present study, the SMILES representations of the compounds 4′,4-dihydroxy-3′-methoxychalcone and 2′,4-dihydroxy-3-methoxychalcone were evaluated using SwissADME (**Table 1**) to examine key parameters relevant to oral drug development, including aqueous solubility, predicted gastrointestinal absorption, and bioavailability [19].

Table 1 RCSB file IDs of Selected Receptors, Native Ligands, and Positive Control Ligands.

No	Protein/Receptor	PDB ID	Native Ligand (Ligand ID)	Ligand name/Description	Positive control ligand
1	Mcl-1	5FC4	Q2G	(S)-4-(3-(2-chloro-4-(methylsulfonyl)phenoxy)propylamino)-N-(4-(pyridin-2-yl)benzyl)benzamide	S63845
2	Brag-1(BAG-1)	6FAE	ADP	Adenosine diphosphate	ATP
3	Bfl-1 (A1)	3I1H	QIN	2-(3,5-Dimethyl-1H-pyrrol-2-yl)-1H-benzimidazole	BI-97C1 (Sabutoclax)
4	Bcl-xL	7LH7	9LA	ABT-737 analogue (BH3 mimetic)	ABT-263 (Navitoclax)
5	Bcl-w	1ZY3	PEP	BH3 peptide from Bim	WEHI-539
6	Bcl-2	6QGG	85V	Venetoclax (ABT-199)	ABT-199 (Venetoclax)

Preparation of target proteins

Apoptosis is a strictly controlled biological process that eliminates unneeded or damaged cells and is crucial for preserving cellular homeostasis [20]. Regulation of this process is largely mediated by the BCL-2 family of proteins, consisting of anti-apoptotic components including BCL-2, BCL-xL, BCL-w, MCL-1, and A1/BFL-1. It functions through both intrinsic and extrinsic routes. and pro-apoptotic proteins (including BAX and BID); the equilibrium between these groups is essential for healthy cell function [20]. The docking targets for this investigation were BCL-2, BAX, BCL-xL, BCL-w, MCL-1, and BRAG-1. Before docking analysis, their three-dimensional structures were retrieved from the RCSB Protein Data Bank (**Table 1**) and pr0cessed by removing native ligands and crystallographic water molecules.

Molecular docking analysis

Computer-aided drug discovery (CADD) is commonly used to study protein-ligand interactions in molecular docking analyses [21,22]. In this study, CB-Dock2 was employed to perform automated blind docking of 4′,4-dihydroxy-3′-methoxychalcone and 2′,4-dihydroxy-3-methoxychalcone against selected anti-apoptotic proteins, namely BCL-2, BCL-w, BCL-xL, BRAG-1, BFL-1, and MCL-1. The resulting ligand-protein complexes were subsequently analyzed and visualized using UCSF Chimera [22,23].

Interaction analysis

Protein-ligand interactions and amino acid residues involved in binding were analyzed using Discovery Studio Visualizer [24]. Hydrogen bonding and hydrophobic interactions were identified and compared with those observed in native ligand-protein complexes to evaluate binding site similarity.

Energy minimization

The docked protein-ligand complexes were subjected to energy minimization using Swiss-PDB Viewer to determine their structural stability [25]. Force field energy values before and after minimization were recorded to evaluate structural relaxation and stability.

***In silico* toxicity prediction**

The ProTox-II web platform was employed to estimate the acute toxicity profiles of the two chalcone derivatives [26]. The SMILES notation of each compound was uploaded to predict LD_{50} values and toxicity classifications using established machine learning models.

Results and discussion

Preparation of 2',4-dihydroxy-3-methoxychalcone

2',4-Dihydroxy-3-methoxychalcone was obtained (**Figure 2**) through Claisen-Schmidt condensation reaction to afford a yellow crystalline solid with a melting temperature of 148 - 150 °C and an isolated yield of 34%. Mass spectrometric analysis revealed a molecular ion peak at *m/z* 270.1, consistent with the expected molecular mass. The compound structur was verified using FTIR, ^{1}H-NMR, and ^{13}C-NMR spectroscopy. FTIR (KBr) cm^{-1} : 3426 (OH), 3066 (C-H aromatic), 1605 (C=O), 1513 (C=C), 1121 (-OCH_3); MS m/z: 270 (M+); ^{1}H-NMR (Methanol-d4) (δ ppm): 3.95 (s, 3H, -OCH3), 6.86 (d, J= 6,5 Hz, 1H, Ar-H), 6.98 (m, 2H, Ar-H), 7.26 (dd, 1H, J= 2; J=2, Ar-H), 7.41 (s, 1H, Ar-H), 7.50 (t, 1 H, Ar-H), 7.76 (d, 1H, J=15.5 Hz, Hα), 7.87 (d, 1 H, J=15.5, Hβ), 8.17 (d, 1 H, J= Hz, Ar-H); ^{13}C-NMR (Methanol-d4) (δ ppm): 56.69, 112.47, 116.74, 118.51, 119.15, 120.23, 125.60, 128.35, 131.49, 137.28, 147.61, 149.65, 151.53, 164.56, 195.64.

The ^{1}H-NMR spectrum (Methanol-d_4) displayed a methoxy singlet at δ 3.95 ppm (3H), along with multiple aromatic proton signals in the range of δ 6.86 - 8.17 ppm. Notably, two doublets at δ 7.76 ppm (1H, J = 15.5 Hz) and δ 7.87 ppm (1H, J = 15.5 Hz) were assigned to the olefinic Hα and Hβ protons, respectively, confirming the presence of a trans (E)-α,β-unsaturated system. The ^{13}C-NMR spectrum showed a characteristic carbonyl signal at δ 195.64 ppm, along with signals corresponding to aromatic, olefinic, and methoxy carbons. These spectroscopic features unequivocally confirm the successful synthesis of the target chalcone.

The spectroscopic data are generally consistent with those reported by Mahesh *et al.* [6] however, in contrast to their observations, the present study clearly resolves the olefinic proton signals with a large coupling constant (J = 15.5 Hz), allowing unambiguous

assignment of the trans (E) configuration. Minor differences in chemical shifts may be attributed to solvent effects (Methanol-d_4 vs. other solvents) and substituent-induced electronic variations.

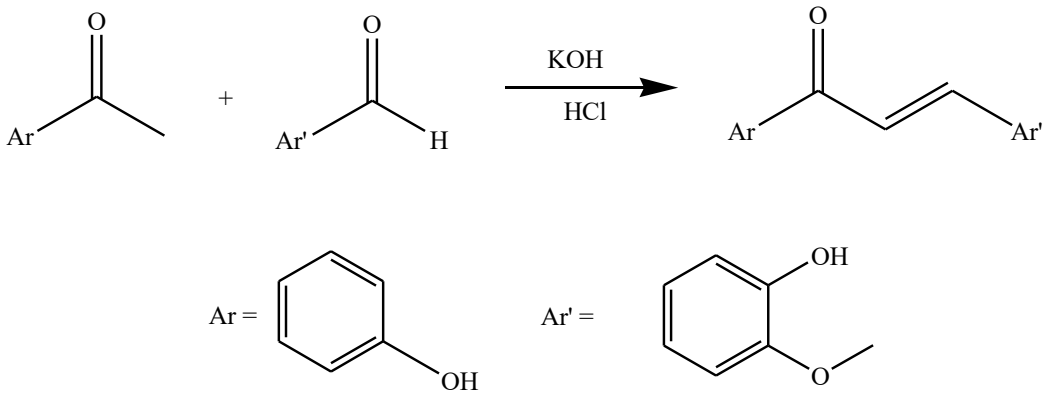


Figure 2 Synthesis reaction of 2',4-**d**ihydroxy-3-methoxychalcone. The target chalcone was prepared through KOH-catalyzed Claisen-Schmidt condensation of the appropriate acetophenone derivative and aromatic aldehyde, followed by acidification with HCl. This reaction produces the α,β-unsaturated ketone framework characteristic of chalcones. The synthesized compound was used for comparative computational assessment with its structural chalcone isomer.

Drug-likeness and ADME evaluation of the ligand

The produced 2′,4-dihydroxy-3-methoxychalcone displayed physicochemical and predicted pharmacokinetic characteristics consistent with drug-like compounds (**Table 2**), with physicochemical parameters consisting of a molecular massa of 312 Da, five hydrogen bond donors goups, six hydrogen bond acceptors groups, and a predicted Log P of −0.053. These parameters comply with Lipinski's rule of 5. Although both chalcone isomers share comparable physicochemical properties, 2′,4-dihydroxy-3-methoxychalcone exhibited a lower predicted aqueous solubility (Log S = −4.39) than its positional isomer (Log S = −3.28). Both compounds showed high predicted gastrointestinal absorption and an identical bioavailability score of 0.55. Previous studies have reported cytotoxic activity of 2′,4-dihydroxy-3-methoxychalcone against HeLa and WiDr cancer cell line, and chalcone derivatives have been associated with apoptosis-related signaling pathways [6]. Differences in hydroxyl substitution patterns may therefore influence solubility and biological behavior, supporting further mechanistic and experimental investigation [12,13].

Table 2 Drug Likeness and ADME Parameters.

No	Parameter	2',4-dihydroxy-3-methoxychalcone	4',4-dihydroxy-3'-methoxychalcone
1	Molecular mass	312.000000	312.000000
2	hydrogen bond donor	5	5
3	hydrogen bond acceptors	6	6
4	Log P	–0.053101	–0.053101
5	Molar Refractivity	77.145782	77.145782
6	Log S (Ali)	–4.39	–3.28
7	Solubility in H_2O	Moderately Soluble	Soluble
8	G.I Absorption	High	High
9	Bioavailability Score	0.55	0.55

Docking Study of 4',4-dihydroxy-3'-methoxychalcone and 2',4-dihydroxy-3-methoxychalcone Against Antiapoptotic Proteins via CB-Dock2

Molecular docking of 2′,4-dihydroxy-3-methoxychalcone against selected anti-apoptotic Bcl-2 family proteins (**Table 3**, **Figure 3**) showed favorable binding affinities, with Vina scores ranging from −6.3 kcal/mol for Bfl-1 to −9.3 kcal/mol for Bcl-xL. Among the evaluated targets, Bcl-xL exhibited the strongest interaction. Hydrogen bonding was observed with Bcl-xL (SER106, ARG139), Brag-1 (SER615, THR592, GLN601), Bfl-1 (ASN142, GLU5), and Bcl-w (LEU67, ALA64), which are residues previously reported to contribute to binding stability and selectivity in protein-ligand interactions [13,27]**.** Interactions with Mcl-1 and Bcl-2 were predominantly hydrophobic, involving residues such as PHE270 and MET250 (Mcl-1) and PHE104 and TYR108 (Bcl-2), consistent with earlier docking and structural studies [28]. Comparison with native ligand binding sites revealed overlapping residues, including MET250 in Mcl-1 and TYR108 in Bcl-2, suggesting occupation of biologically relevant binding pockets [12]. These observations are in agreement with previous studies reporting chalcone interactions with Bcl-2 family proteins [4,5].

Table 3 Binding affinity (Vina score) and Amino acid interactions of 2',4-Dihydroxy-3-methoxychalcone with target proteins and corresponding native ligands.

Protein/ Receptors	Binding Energy (Vina Score)	Docking coordinates identified by CB-Dock	Amino Acids Residues Interacting with 2',4-dihydroxy-3-methoxychalcone (DSV)	Hydrogen bonds between 2',4-dihydroxy-3-methoxychalcone and protein (DSV)	Amino Acids Residues Participating in Native Ligand Binding and heteroatom Interactions (DSV)
Mcl-1 (5FC4)	–7.4	4, 4, 14	LEU A: 246, MET A: 250, PHE A: 270	Nil	MET A: 250, MET A: 231, PHE A: 270, LEU A: 267, VAL A: 249, VAL A: 253, ALA A: 227, PHE A: 228, THR A: 266, ARG A: 263
Brag-1 (6FAE)	–7.5	7, 72, –31	SER A: 615, PRO B: 47, GLN A: 601, THR A: 592, ASP A: 595, ILE B: 46, ARG A: 494	SER A: 615, THR A: 592, GLN A: 601	LYS B: 73, ARG A: 565
Bfl-1 (3I1H)	–6.3	4, –10, –2	ASN A: 142, GLU A: 5, ILE A: 134	ASN A: 142, GLU A: 5	No native ligand was identified in the crystal structure available in the RCSB database.
Bcl-xl (7LH7)	–9.3	7, –11, –11	LEU A: 108, SER A: 106, PHE A: 105, ARG A: 139, ALA B: 104, ALA A: 142, ARG A: 102, PHE A: 146	SER A: 106, ARG A: 139	TYR A: 195, GLU A: 96. VAL A: 141, TYR A: 101, PHE A: 191, ASN A: 136, PHE A: 97, ALA A: 142, LEU A: 108, PHE A: 146, ARG A: 102, ALA A: 149, SER A: 106, LEU A: 130, ALA B: 104, PHE A: 105, ARG A: 139, GLY A: 138
Bcl-w (1ZY3)	–7.7	–8, –9, –4	VAL A: 81, ARG A: 77, PHE A: 78, ALA A: 64, ALA A: 104, LEU A: 105, LEU A: 67	LEU A: 67, ALA A: 64	No native ligand was identified in the crystal structure available in the RCSB database.
Bcl-2 (6QGG)	–7.6	–15, 17, –6	TYR A: 108, LA A: 149, PHE A: 104, TYR A: 202, ALA A: 100, PHE A: 198, VAL A: 148	Nil	ASP A: 103, TYR A: 202, GLY A: 145, VAL A: 148, PHE A: 104, TYR A: 108, ASP A: 111, LEU A: 137, VAL A: 156, MET A: 115, PHE A: 112, ALA A: 149

Molecular docking analysis of 4′,4-dihydroxy-3′-methoxychalcone against anti-apoptotic Bcl-2 family proteins (**Table 4**, **Figure 4**) revealed binding affinities with Vina scores ranging from −6.3 kcal/mol for Bfl-1 to −9.5 kcal/mol for Bcl-xL. Among the evaluated targets, Bcl-xL exhibited the strongest interaction. Hydrogen bonding was observed in complexes with Brag-1 (SER448, GLN450) and Bfl-1 (GLU5), contributing to binding specificity, whereas no hydrogen bonds were detected in the Bcl-xL complex, indicating that hydrophobic and van der Waals interactions likely dominate complex stabilization [13,27]. Analysis of interacting residues showed substantial overlap with native ligand binding sites (**Figure 5**), including MET250 and ARG263 in Mcl-1, as well as ALA100 and PHE104 in Bcl-2, suggesting occupation of biologically relevant binding pockets [12,28]. Compared with 2′,4-dihydroxy-3-methoxychalcone, the 4′,4-dihydroxy-3′-methoxychalcone displayed comparable or slightly lower binding affinities while maintaining similar interaction patterns. These observations indicate that hydroxyl positional isomerism influences docking behavior and interaction profiles, consistent with previously reported structure-activity relationship studies on chalcone derivatives [4,5].

Table 4 Binding affinity (Vina score) and Amino acid Interactions of 4’,4-dihydroxy-3’-methoxychalcone with target proteins and corresponding native ligands.

Protein/ Receptors	**Binding Energy (Vina Score)**	**Docking coordinates identified by CB-Dock**	**Amino Acids Residues Interacting with 4’,4-dihydroxy-3’-methoxychalcone (DVS)**	**Hydrogen bonds between 4’,4-dihydroxy-3’-methoxychalcone and protein (DVS)**	**Amino Acids Residues Participating in Native Ligand Binding and heteroatom Interactions (DSV)**
Mcl-1 (5FC4)	–7.2	4, 4, 14	LEU A: 246, LEU A: 267, PHE A: 270, MET A: 250, VAL A: 253, ARGA: 263	ARG A: 263	MET A:250, MET A:231, PHE A:270, LEU A:267, VAL A:249, VAL A:253, ALA A:227, PHE A:228, THR A:266, ARG A:263
Brag-1 (6FAE)	–7.6	9, 72, –31	GLN A: 450, PRO B: 47, ILE B: 46, ARG A: 494, SER A: 598, SER A: 448, VAL A: 597, PRO A: 617	SER A: 448, GLN A: 450	LYS B:73, ARG A:565
Bfl-1 (3I1H)	–6.3	23, –15, 2	GLU A: 5, ARG A: 135, GLU A: 141, ILE A: 134	GLU A: 5	No native ligand was identified in the crystal structure available in the RCSB database.
Bcl-xl (7LH7)	–9.5	7, –11, –11	ALA A: 104, ARG B: 139, PHE B: 105, LEU B: 130, PHE B: 146, ARG B: 102, LEU B: 108	Nil	TYR A:195, GLU A:96. VAL A:141, TYR A:101, PHE A:191, ASN A:136, PHE A:97, ALA A:142, LEU A:108, PHE A:146, ARG A:102, ALA A:149, SER A:106, LEU A:130, ALA B:104, PHE A:105, ARG A:139, GLY A:138

Protein/ Receptors	Binding Energy (Vina Score)	Docking coordinates identified by CB-Dock	Amino Acids Residues Interacting with 4',4-dihydroxy-3'-methoxychalcone (DVS)	Hydrogen bonds between 4',4-dihydroxy-3'-methoxychalcone and protein (DVS)	Amino Acids Residues Participating in Native Ligand Binding and heteroatom Interactions (DSV)
Bcl-w (1ZY3)	–7.5	–8, –9, –4	ARG A: 77, VAL A: 81, PHE A: 78, HIS A: 68, ALA A: 64, GLU A: 108	GLU A: 108	No native ligand was identified in the crystal structure available in the RCSB database.
Bcl-2 (6QGG)	–7.2	–15, 17, –6	ALA A: 100, PHE A: 104, TYR A: 202, VAL A: 148, TYR A: 108, ALA A: 149	ALA A: 100, PHE A: 104	ASP A: 103, TYR A: 202, GLY A: 145, VAL A: 148, PHE A: 104, TYR A: 108, ASP A: 111, LEU A: 137, VAL A: 156, MET A: 115, PHE A: 112, ALA A: 149

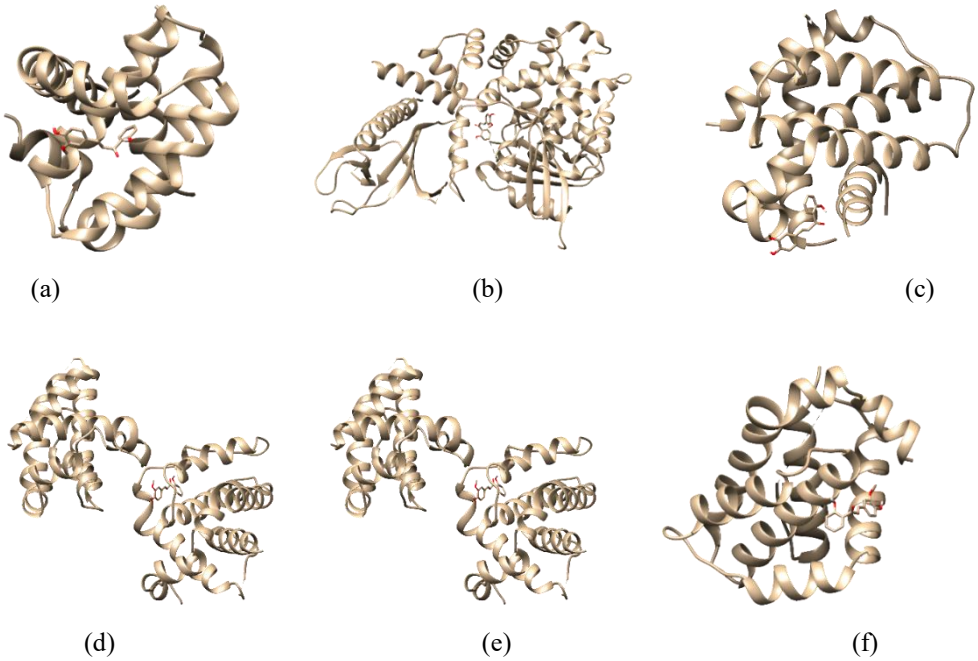


Figure 3 Molecular docking interactions between 2',4-dihydroxy-3-methoxychalcone and selected target proteins: (a) Interaction of Mcl-1 protein with the ligand 2',4-dihydroxy-3-methoxychalcone; (b) Interaction of Brag-1 protein with the ligand 2',4-dihydroxy-3-methoxychalcone; (c) Interaction of Bfl-1 protein with the ligand 2',4-dihydroxy-3-methoxychalcone; (d) Interaction of Bcl-xl protein with the ligand 2',4-dihydroxy-3-methoxychalcone; (e) Interaction of Bcl-w protein with the ligand 2',4-dihydroxy-3-methoxychalcone; and (f) Interaction of Bcl-2 protein with the ligand 2',4-dihydroxy-3-methoxychalcone.

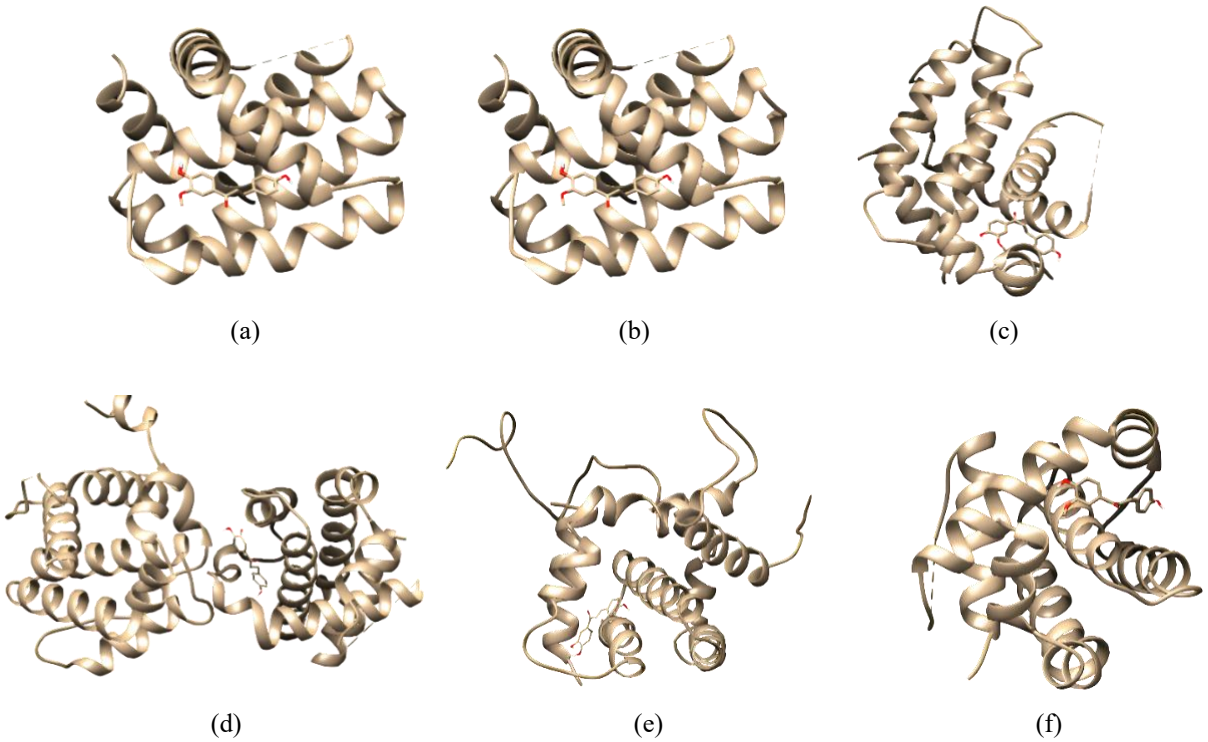
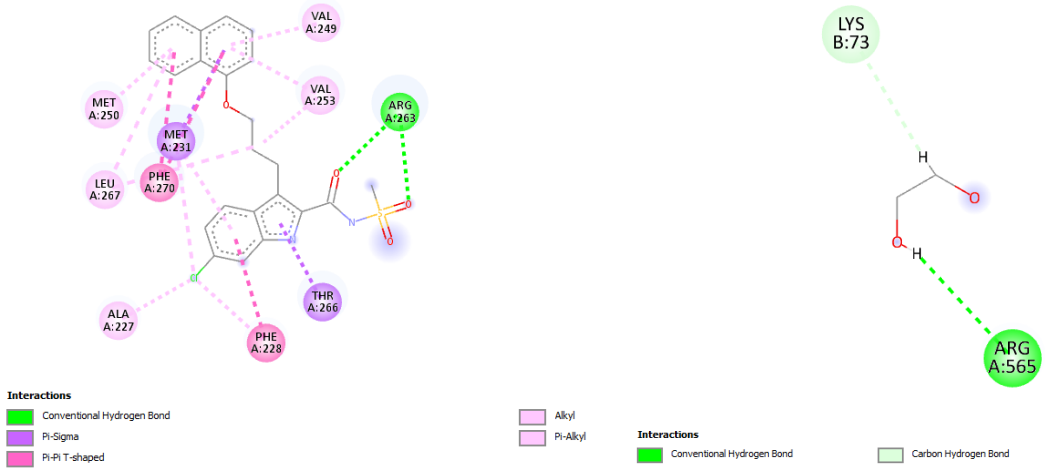
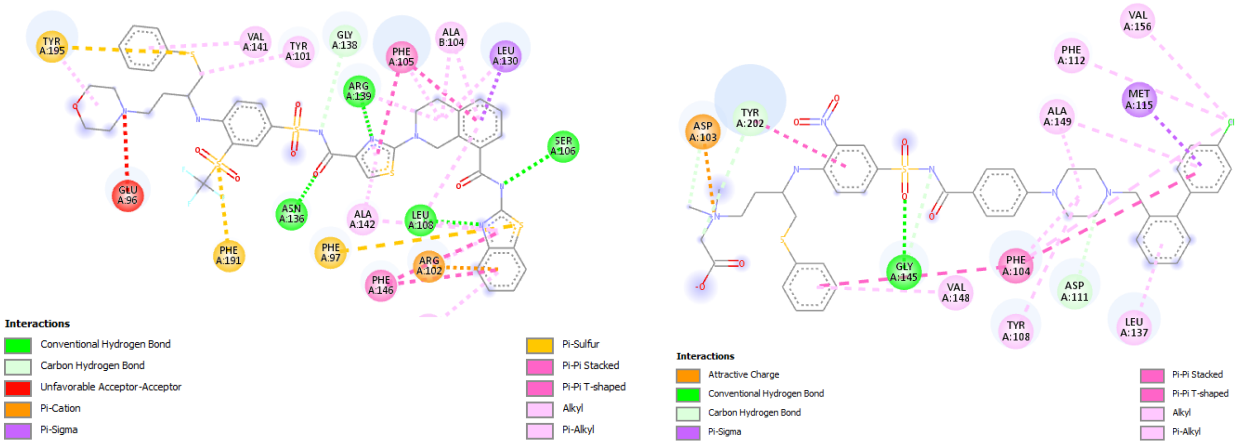


Figure 4 Molecular docking interactions between 4',4-dihydroxy-3'-methoxychalcone and selected target proteins: (a) Interaction of Mcl-1 protein with the ligand 4',4-dihydroxy-3'-methoxychalcone; (b) Interaction of Brag-1 protein with the ligand 4',4-dihydroxy-3'-methoxychalcone; (c) Interaction of Bfl-1 protein with the ligand 4',4-dihydroxy-3'-methoxychalcone; (d) Interaction of Bcl-xl protein with the ligand 4',4-dihydroxy-3'-methoxychalcone; (e) Interaction of Bcl-w protein with the ligand 4',4-dihydroxy-3'-methoxychalcone; and (f) Interaction of Bcl-2 protein with the ligand 4',4-dihydroxy-3'-methoxychalcone.

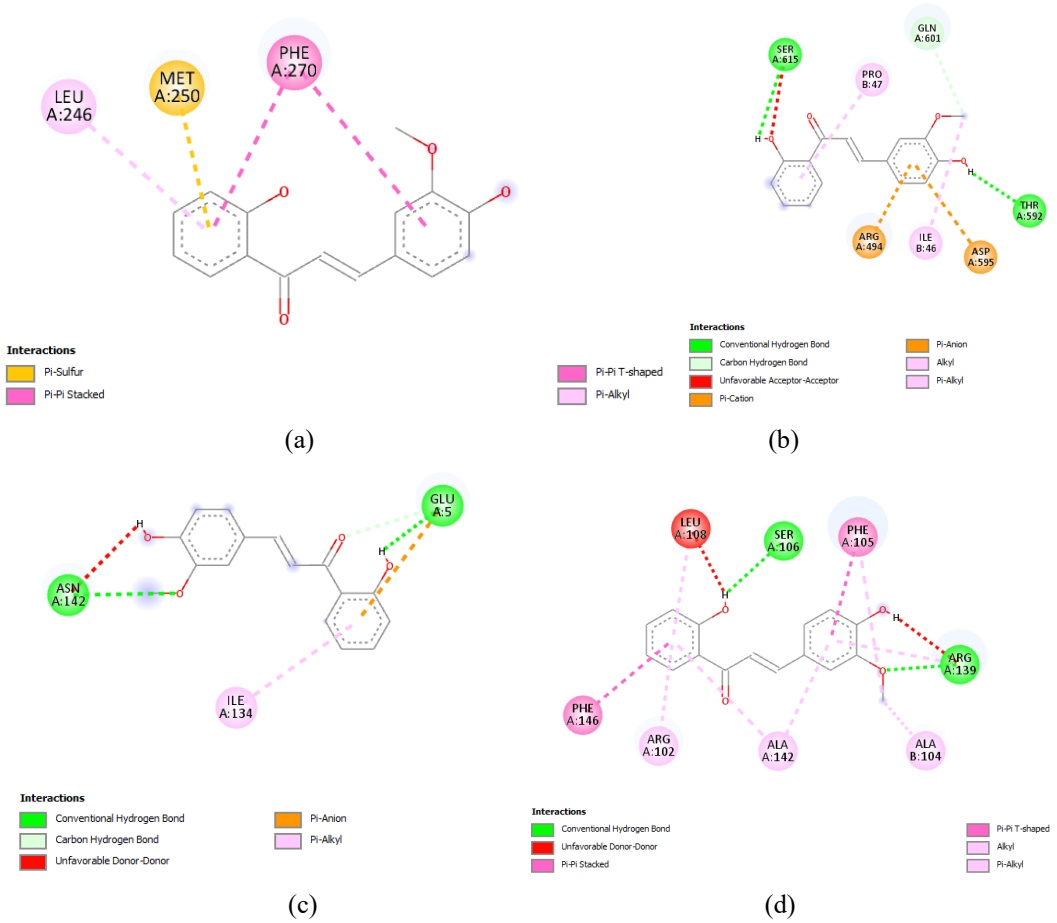


(a) (b)



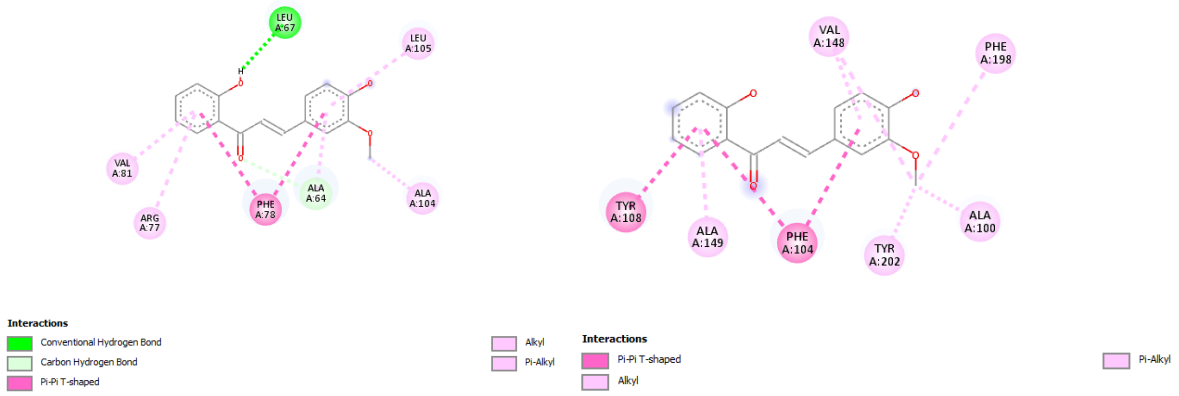
(c) (d)

Figure 5 Amino acid side-chain interactions of native ligands at the binding sites of apoptotic proteins visualized using the DSV tool. The figure presents two-dimensional interaction profiles showing the binding orientation of each native ligand and the amino acid residues involved in ligand stabilization within the protein binding pocket. (a) Native ligand interaction with Mcl-1, showing the hydrogen-bonding and hydrophobic interaction pattern within the Mcl-1 binding site. (b) Native ligand interaction with Brag-1, illustrating the main ligand-residue contacts involved in binding stabilization. (c) Native ligand interaction with Bcl-xL, displaying a broader interaction network between the native ligand and surrounding amino acid residues. (d) Native ligand interaction with Bcl-2, showing the interaction pattern of the native ligand within the Bcl-2 binding pocket.



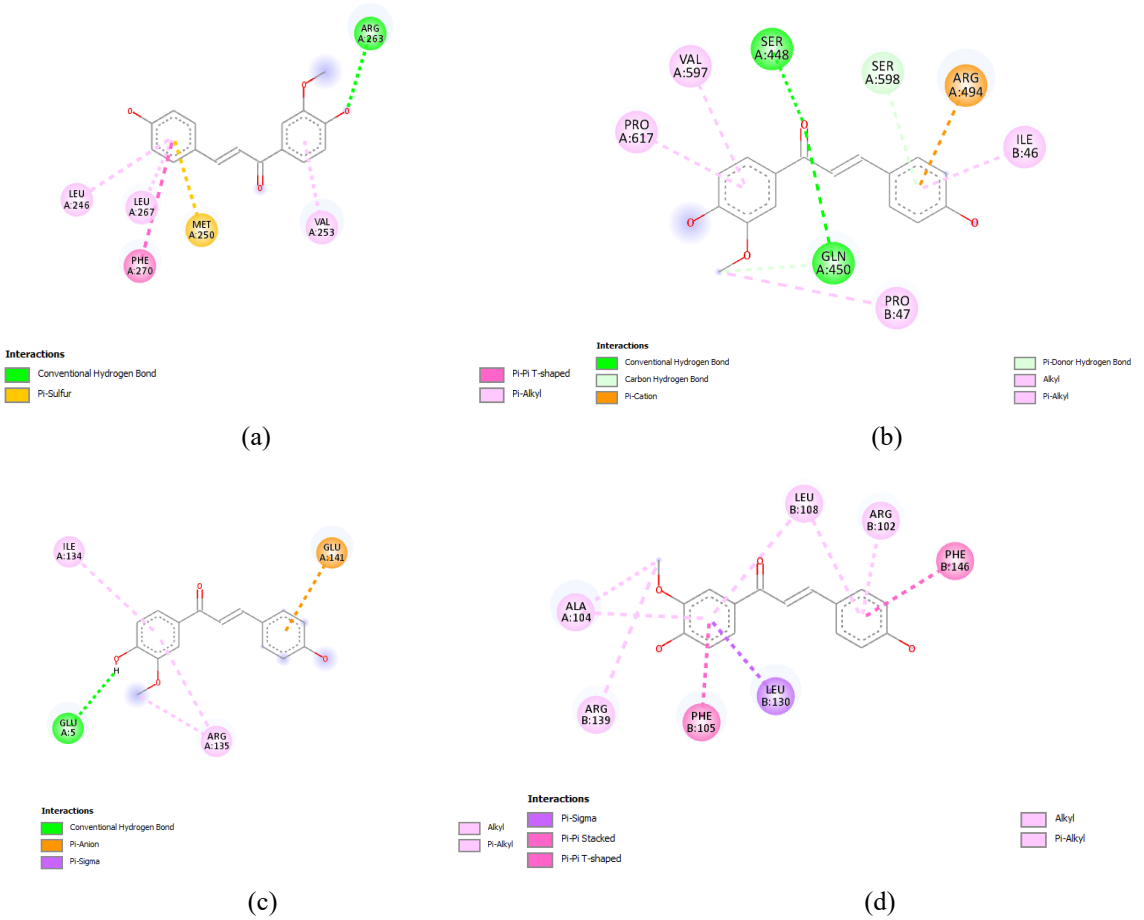
(a) (b)

(c) (d)



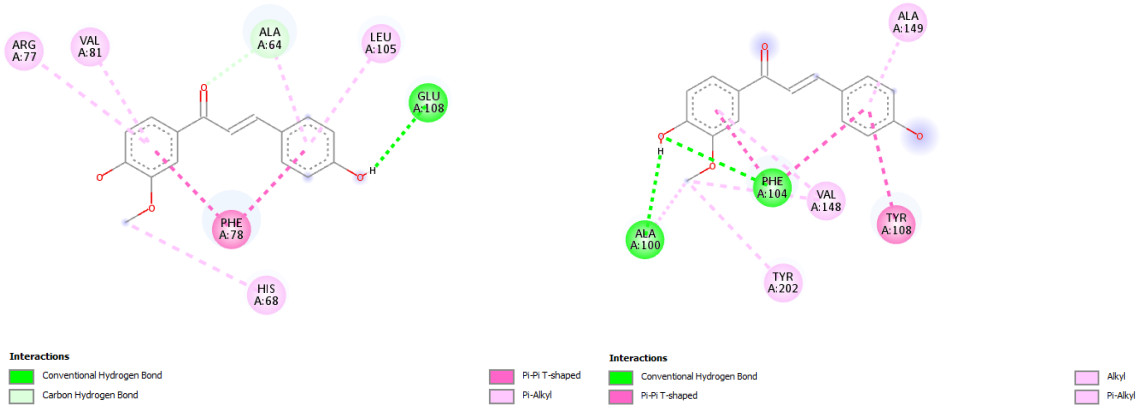
(e) (f)

Figure 6 Amino acid side-chain interactions of 2′,4-dihydroxy-3-methoxychalcone at the binding sites of selected apoptotic proteins visualized using the DSV tool. The figure presents two-dimensional interaction profiles showing the binding orientation of 2',4-dihydroxy-3-methoxychalcone and the amino acid residues involved in ligand stabilization within each protein binding pocket. (a) Interaction of the ligand with Mcl-1, showing π-related and hydrophobic contacts within the binding site. (b) Interaction of the ligand with Brag-1, illustrating hydrogen-bonding, carbon-hydrogen bonding, electrostatic, and hydrophobic contacts. (c) Interaction of the ligand with Bfl-1, showing hydrogen-bonding and hydrophobic interactions that support ligand binding. (d) Interaction of the ligand with Bcl-xL, displaying hydrogen-bonding and π-related interactions with surrounding residues. (e) Interaction of the ligand with Bcl-w, showing hydrogen-bonding, carbon-hydrogen bonding, and hydrophobic contacts. (f) Interaction of the ligand with Bcl-2, illustrating predominantly hydrophobic and π-related interactions within the binding pocket.



(a) (b)

(c) (d)



(e) (f)

Figure 7 Amino acid side-chain interactions of the structural chalcone isomer at the binding sites of selected apoptotic proteins visualized using the DSV tool. The figure presents two-dimensional interaction profiles showing the binding orientation of the structural chalcone isomer and the amino acid residues involved in ligand stabilization within each protein binding pocket. (a) Interaction of the ligand with Mcl-1, showing hydrogen-bonding and π-related interactions within the binding site. (b) Interaction of the ligand with Brag-1, illustrating hydrogen-bonding, carbon-hydrogen bonding, π-cation, alkyl, and π-alkyl contacts. (c) Interaction of the ligand with Bfl-1, showing hydrogen-bonding, π-anion, π-sigma, alkyl, and π-alkyl interactions. (d) Interaction of the ligand with Bcl-xL, displaying π-sigma, π-π stacked, π-π T-shaped, alkyl, and π-alkyl interactions. (e) Interaction of the ligand with Bcl-w, showing hydrogen-bonding, carbon-hydrogen bonding, π-π T-shaped, and π-alkyl contacts. (f) Interaction of the ligand with Bcl-2, illustrating hydrogen-bonding, π-π T-shaped, alkyl, and π-alkyl interactions within the binding pocket.

Energy minimization

Energy minimization analysis of the complexes formed by 2′,4-dihydroxy-3-methoxychalcone and 4′,4-dihydroxy-3′-methoxychalcone with Bcl-2 family proteins showed consistent energy trends across all targets (**Table 5**). In all cases, minimized energies were substantially lower than the corresponding force field energies, indicating the formation of energetically favorable and stable conformations after optimization [29]. For example, the 2′,4-dihydroxy-3-methoxychalcone-Bcl-xL complex exhibited a decrease in energy from −13,417.5 kJ/mol to −16,785.2 kJ/mol following minimization. Comparable minimized energy values for both ligands suggest that hydroxyl positional isomerism has a limited effect on the overall thermodynamic stability of the ligand-protein complexes during molecular mechanics optimization. These results support the stability and reliability of the predicted docking poses [13,26], and highlight the role of energy minimization in refining ligand-protein interactions to conformations relevant for subsequent pharmacological evaluation [28,30].

Table 5 Comparison of Force Field Energy and Energy after Minimization.

Ligand	Protein	Force field energy (kJ/mol)	Minimized energy (kJ/mol)
2’,4-dihydroxy-3-methoxychalcone	Mcl-1	–5986.007	–8567.683
	Brag-1	–24272.641	–32597.195
	Bfl-1	–7257.693	–9542.819
	Bcl-xl	–13417.518	–16785.162
	Bcl-w	–6627.017	–8770.945
	Bcl-2	–5600.351	–8233.023

4’,4-dihydroxy-3’-methoxychalcone	Mcl-1	–5986.007	–8567.683
	Brag-1	–24272.641	–32597.195
	Bfl-1	–7257.693	–9542.819
	Bcl-xl	–13417.518	–16785.162
	Bcl-w	–6627.017	–8770.945
	Bcl-2	–5600.351	–8233.023

Toxicity assay

In silico toxicity assessment indicated that both 2′,4-dihydroxy-3-methoxychalcone and 4′,4-dihydroxy-3′-methoxychalcone showed an identical predicted LD_{50} value of 2580 mg/kg, corresponding to toxicity class 5 [31]. This result suggests that both chalcone compounds have low predicted acute toxicity. Minor differences were observed in the prediction metrics, with average similarity and prediction accuracy values of 77.84% and 69.26% for 2′,4-dihydroxy-3-methoxychalcone, and 85.73% and 70.97% for 4′,4-dihydroxy-3′-methoxychalcone, respectively. These differences may be associated with the positional variation of hydroxy and methoxy substituents between the two chalcone isomers. Overall, the predicted toxicity data indicate comparable safety profiles for both compounds. However, further *in vivo* toxicity studies are required to validate these computational predictions and support their potential preclinical development [32-35].

Table 6 Predicted toxicity profiles of 2′,4-dihydroxy-3-methoxychalcone and its structural chalcone isomer.

Compound	Predicted LD_{50}(mg/Kg)	Toxicity class	Average similarity (%)	Prediction accuracy (%)	Interpretation
2′,4-Dihydroxy-3-methoxychalcone	2580	Class 5	77.84	69.26	Low predicted acute toxicity
4′,4-Dihydroxy-3′-methoxychalcone	2580	Class 5	85.73	70.97	Low predicted acute toxicity

Conclusions

This study indicates that 2′,4-dihydroxy-3-methoxychalcone was successfully synthesized and structurally characterized. The produced chemical and its positional isomer interact favorably with anti-apoptotic Bcl-2 family members, especially Bcl-xL, according to computational research, producing stable ligand-protein complexes following energy minimization. In silico toxicity prediction suggested low acute toxicity for both chalcones. Overall, the findings provide a computational basis for futher experiemental investigation of hydroxy-methoxychalcone derivatives in studies related to apoptosis-regulating targets.

Acknowledgements

The authors gratefully acknowledge the financial support provided by Ministry of Research, Technology, and Hinger Education (Republic of Indonesia) through the doctoral dissertation research (PDD) grant contract number 02035/UN4.22.2/PT.01.03/2024. The authors also thank the organic chemistry laboratory of Hasanuddin University, Sulawesi Selatan 90245, Indonesia and UIN Alauddin Makassar, Sulawesi Selatan 92113, Indonesia for providing the facilities and technical support essential to this study.

Declaration of Generative AI in Scientific Writing

The authors declare that generative artificial intelligence (AI) tools were used solely to assist in improving the clarity, grammar, and readability of the manuscript. The use of these tools was conducted under full human supervision, and all scientific content, interpretations, and conclusions were critically reviewed and approved by the authors. Generative AI tools were

not used to generate original research data, analyses, or conclusions and were not listed as authors or co-authors. The authors take full responsibility for the integrity and accuracy of the content presented in this manuscript.

CRediT Author Statement

Arfiani Nur: contributed to conceptualization, methodology, investigation, data curation, and writing of the original draft. **Nunuk Hariani Soekamto**: contributed to conceptualization, supervision, validation, and writing—review and editing. **Bambang Purwono:** contributed to methodology, formal analysis, and writing—review and editing. **Herlina Rasyid**: contributed to validation, data curation, and writing—review and editing. **Ummi Zahra and Aisyah**: contributed to investigation and data curation. **Artati**: contributed to resources and methodological support. **Andi Nur Fitriani**: contributed to formal analysis and visualization. **Fadliah and M. Yasser**: contributed to computational analysis and software. **Muharram**: contributed to resources and validation. **Paulina Taba**: contributed to supervision and writing—review and editing. **Indah Raya**: contributed to supervision and project administration. **Abdul Wahid Wahab:** contributed to supervision. **Najah Baroud**: contributed to validation and writing—review and editing.

References

[1] SM Villa, J Heckman and D Bandyopadhyay. Medicinally privileged natural chalcones: Abundance, mechanisms of action, and clinical trials. *International Journal of Molecular Sciences* 2024; **25(17)**, 9623.

[2] I Baramaki, MD Altıntop, R Arslan, FA Altınok, A Özdemir, I Dallali, A Hasan and NB Türkmen. Design, synthesis, and *in vivo* evaluation of a new series of indole-chalcone hybrids as analgesic and anti-inflammatory agents. *ACS Omega* 2024; **9(10)**, 12175-12183.

[3] M Rudrapal, J Khan, AAB Dukhyil, RMII Alarousy, EI Attah, T Sharma, SJ Khairnar and AR Bendale. Chalcone scaffolds, bioprecursors of flavonoids: Chemistry, bioactivities, and pharmacokinetics. *Molecules* 2021; **26(23)**, 7177.

[4] AE Varakutin, EA Muravsky, DV Tsyganov, IY Shinkarev, AI Samigullina, TS Kuptsova, RN Chuprov-Netochin, AV Smirnova, AA Khomutov, SV Leonov, MN Semenova and VV Semenov. Synthesis of chalcones with methylenedioxypolymethoxy fragments based on plant metabolites and study of their antiproliferative properties. *Russian Chemical Bulletin* 2023; **72**, 1632-1647.

[5] J Moreira, J Almeida, L Saraiva, H Cidade and M Pinto. Chalcones as promising antitumor agents targeting the p53 pathway: An overview and insights in drug-likeness. *Molecules* 2021; **26(12)**, 3737.

[6] S Matsjeh, RT Swasono, C Anwar, EN Solikhah and E Lestari. Synthesis of 2',4-dihydroxy-3-methoxychalcone and 2',4',4-trihydroxy-3-methoxychalcone as a candidate anticancer against cervical (WiDr), colon (HeLa), and breast (T47d) cancer cell lines *in vitro*. *AIP Conference Proceedings* 2017; **1823**, 020048.

[7] S Qian, Z Wei, W Yang, J Huang, Y Yang and J Wang. The role of BCL-2 family proteins in regulating apoptosis and cancer therapy. *Frontiers in Oncology* 2022; **12**, 985363.

[8] M Vogler, Y Braun, VM Smith, MA Westhoff, RS Pereira, NM Pieper, M Anders, M Callens, T Vervliet, M Abbas, S Macip, R Schmid, G Bultynck and MJS Dyer. The BCL2 family: From apoptosis mechanisms to new advances in targeted therapy. *Signal Transduction and Targeted Therapy* 2025; **10**, 91.

[9] N Mukherjee, J Sheetz and YG Shellman. Targeting the BCL2 family: Advances and challenges in BH3 mimetic-based therapies. *International Journal of Molecular Sciences* 2025; **26(20)**, 9859.

[10] Y Jia, L Han, CL Ramage, Z Wang, CC Weng, L Yang, S Colla, H Ma, W Zhang, M Andreeff, N Daver, N Jain, N Pemmaraju, K Bhalla, S Mustjoki, P Zhang, G Zheng, D Zhou, Q Zhang and M Konopleva. Co-targeting BCL-XL and BCL-2 by PROTAC 753B eliminates leukemia cells and enhances efficacy of chemotherapy by targeting senescent cells. *Haematologica* 2023; **108(10)**, 2626-2638.

[11] D Ćirin and V Krstonošić. New insights into binding of natural chalcones to Bcl-2, Bcl-xL and Mcl-1 anti-apoptotic proteins. *Journal of Molecular Structure* 2021; **1241**, 130700.

[12] S Zhang, T Li, L Zhang, X Wang, H Dong, L Li, D Fu, Y Li, X Zi, HM Liu, Y Zhang, H Xu and CY Jin. Retracted article: A novel chalcone derivative induces apoptosis through ROS dependent DR5 up-regulation in gastric cancer cells. *Scientific Reports* 2017; **7**, 9873.

[13] X Wang, Y Liang, B Zhang, L He, W Li, W Zhang, C Li, L Luo, T Umar, H Feng and C Qiu. 2′-Hydroxychalcone induces autophagy and apoptosis in breast cancer cells via inhibition of the NF-κB signaling pathway: *In vitro* and *in vivo* studies. *Nutrients* 2024; **16(4)**, 514.

[14] N Seflini, PR Triananda, F Kurniadewi, Zulhipri and H Dianhar. Synthesis of vanillin-derived chalcone using microwave irradiation method. *AIP Conference Proceedings* 2024; **2982**, 040011.

[15] NM O'Boyle, M Banck, CA James, C Morley, T Vandermeersch and GR Hutchison. Open Babel: An open chemical toolbox. *Journal of Cheminformatics* 2011; **3**, 33.

[16] EF Pettersen, TD Goddard, CC Huang, GS Couch, DM Greenblatt, EC Meng and TE Ferrin. UCSF Chimera—A visualization system for exploratory research and analysis. *Journal of Computational Chemistry* 2004; **25(13)**, 1605-1612.

[17] CA Lipinski. Lead- and drug-like compounds: The rule-of-five revolution. *Drug Discovery Today: Technologies* 2004; **1(4)**, 337-341.

[18] B Jayaram, T Singh, G Mukherjee, A Mathur, S Shekhar and V Shekhar. *Sanjeevini*: A freely accessible web server for target-directed lead molecule discovery. *BMC Bioinformatics* 2012; **13(S17)**, S7.

[19] A Daina, O Michielin and V Zoete. SwissADME: A free web tool to evaluate pharmacokinetics, drug-likeness, and medicinal chemistry friendliness of small molecules. *Scientific Reports* 2017; **7**, 42717.

[20] S Goldar, MS Khaniani, SM Derakhshan and B Baradaran. Molecular mechanisms of apoptosis and their roles in cancer development and treatment. *Asian Pacific Journal of Cancer Prevention* 2015; **16**, 2129-2144.

[21] NS Pagadala, K Syed and J Tuszynski. Software for molecular docking: A review. *Biophysical Reviews* 2017; **9**, 91-102.

[22] Y Liu, M Grimm, WT Dai, MC Hou, ZX Xiao and Y Cao. CB-Dock: A web server for cavity detection-guided protein-ligand blind docking. *Acta Pharmacologica Sinica* 2020; **41**, 138-144.

[23] Q Wu, Z Peng, Y Zhang and J Yang. COACH-D: Improved protein-ligand binding site prediction with refined ligand-binding poses through molecular docking. *Nucleic Acids Research* 2018; **46(W1)**, W438-W442.

[24] BIOVIA. *Visualize Your Science*. BIOVIA, California, 2021.

[25] MU Johansson, V Zoete, O Michielin and N Guex. Defining and searching for structural motifs using DeepView/Swiss-PdbViewer. *BMC Bioinformatics* 2012; **13**, 173.

[26] P Banerjee, AO Eckert, AK Schrey and R Preissner. ProTox-II: A webserver for the prediction of toxicity of chemicals. *Nucleic Acids Research* 2018; **46(W1)**, W257-W263.

[27] GM Morris, R Huey, W Lindstrom, MF Sanner, RK Belew, DS Goodsell and AJ Olson. AutoDock4 and AutoDockTools4: Automated docking with selective receptor flexibility. *Journal of Computational Chemistry* 2009; **30(16)**, 2785-2791.

[28] N Helmi. Identification of therapeutic phytochemicals targeting B-cell lymphoma 2 (BCL2) as anti-acute myeloid leukemia agents: An in-silico approach. *Advances in Life Sciences* 2023; **10(4)**, 670-674.

[29] O Pokharkar, H Lakshmanan, G Zyryanov and M Tsurkan. *In silico* evaluation of antifungal compounds from marine sponges against COVID-19-associated mucormycosis. *Marine Drugs* 2022; **20(3)**, 215.

[30] PC Agu, CA Afiukwa, OU Orji, EM Ezeh, IH Ofoke, CO Ogbu, EI Ugwuja and PM Aja. Molecular docking as a tool for the discovery of molecular targets of nutraceuticals in diseases management. *Scientific Reports* 2023; **13**, 13398.

[31] R Ancuceanu, BE Lascu, D Drăgănescu and M Dinu. *In silico* ADME methods used in the evaluation of natural products. *Pharmaceutics* 2025; **17(8)**, 1002.

[32] CN Cavasotto and V Scardino. Machine learning toxicity prediction: Latest advances in toxicity end points. *ACS Omega* 2022; **7(51)**, 47536-47546.

[33] G Xiong, Z Wu, J Yi, L Fu, Z Yang, C Hsieh, M Yin, X Zeng, C Wu, A Lu, X Chen, T Hou and D Cao. ADMETlab 2.0: An integrated online platform for accurate and comprehensive ADMET predictions. *Nucleic Acids Research* 2021; **49(W1)**, W5-W14.

[34] OECD. *OECD Guidelines for the Testing of Chemicals: Test No. 423: Acute Oral Toxicity—Acute Toxic Class Method*. OECD Publishing, Paris, 2001.

[35] K Savva, M Zachariou, D Kynigopoulos, E Fella, MI Vitali, X Kosofidou, M Spyrou, I Sargiannidou, E Panayiotou, N Dietis and GM Spyrou. Preliminary *in vitro* and *in vivo* insights of *in silico* candidate repurposed drugs for Alzheimer's disease. *Life* 2023; **13(5)**, 1095.